Liquid Crystals
Publication details, including instructions for authors and subscription information:
http://www.informaworld.com/smpp/title~content=t713926090

Investigations of a homologous series of chiral siloxane based dimesogenic compounds

Annett Kaeding; Peter Zugenmaier

Online publication date: 06 August 2010

To cite this Article Kaeding, Annett and Zugenmaier, Peter(1998) 'Investigations of a homologous series of chiral siloxane based dimesogenic compounds', Liquid Crystals, 25: 4, 449 — 457
To link to this Article: DOI: 10.1080/026782998205958
URL: http://dx.doi.org/10.1080/026782998205958

LIQUID CRYSTALS, 1998, VOL. 25, NO. 4, 449–457

Investigations of a homologous series of chiral siloxane based dimesogenic compounds

ANNETT KAEDING and PETER ZUGENMAIER*
Institute of Physical Chemistry, TU Clausthal, Arnold-Sommerfeld-Str. 4,
D-38678 Clausthal-Zellerfeld, Germany

(*Received 23 September 1997; in final form 5 March 1998; accepted 26 May 1998*)

A homologous series of siloxane based dimesogens was synthesized in racemic and enantiomeric form. The flexible part of the core is composed of a central hexamethyltrisiloxane unit and two polymethylene chains of variable length. Increasing the number of methylene units in the core promotes smectic phase behaviour whose polymorphism was studied by polarization optical microscopy. Transitions into metastable phases were detected and investigated by differential scanning calorimetry using different heating rates. Information about the crystallization tendency was obtained from annealing experiments by changing annealing temperature and duration. In contrast to short dimesogenic homologues which predominantly showed monomesogen-like behaviour, polymer-like behaviour was observed for the longer homologues. Small angle X-ray diffraction provided data on the temperature dependence of the smectic layer spacing of mesogens and their corresponding dimesogens linked by the siloxane spacer. No significant differences between the layer spacings of the two classes of compounds were detected which suggests chain folding in the dimesogenic compounds and a similar mesogenic orientation for the mesogens and dimesogens.

1. Introduction

Traditionally, most studies on liquid crystal materials have been carried out on low molar mass compounds on the one hand, or on polymeric materials on the other. Side chain polysiloxanes especially exhibit advantageous properties caused by the high flexibility of the siloxane backbone, e.g. reduced viscosities and low glass transitions [1–3]. Furthermore, liquid crystalline polymers (LCPs) attract great interest for technical applications, for example in the area of reversible information storage and electro-optical devices [4]. Recently new optimized liquid crystal displays have been developed based on the combination of the mechanical advantages of polymers with the electro-optical properties of low molar mass materials. A new class of compounds, which incorporates these ideas, is represented by oligomers. At present, fundamental research in this area is performed on derivatives synthesized in both cyclic and linear molecular geometries [5–9]. Knowledge of the liquid crystal phase behaviour, as well as of the structure of the oligomeric materials, is of general importance, and ideas for improved materials may arise from a comparative study of the monomer–oligomer–polymer sequence. Here, we present a study of the mesomorphic behaviour of a homologous series of linear dimesogens in comparison with their mesogenic precursors. The dimesogens investigated contain two chiral mesogenic units linked by a hexamethyltrisiloxane unit via polymethylene chains of variable length, an unusual mesogenic geometry of a dimesogenic molecule. All homologues were synthesized in enantiomeric and racemic form to investigate the influence of chirality upon special liquid crystal properties and structural parameters. The characterization of the mesophases was carried out by differential scanning calorimetry (DSC) and polarization optical microscopy (POM). Information about the crystallization tendency of the polymer-like dimesogens was derived from different annealing experiments as a function of time and temperature.

Pursuing the goal of mesophase structure determination of liquid crystal compounds, our special interest in this paper is concerned with a study of the principles of mesogenic alignment in siloxane based dimesogens compared with their monomesogenic precursors. As a first step in structure investigation, we have focused our interest on the evolution of the smectic layer spacings as a function of increasing polymethylene chain length in the dimesogens in comparison with those of the corresponding monomesogens.

2. Experimental

A homologous series of dimesogenic compounds based on 4-(2-methylbutyloxy)phenyl-4-alkenyloxybenzoates

*Author for correspondence.

0267–8292/98 $12·00

[10] and a hexamethyltrisiloxane unit has been synthesized in both chiral and racemic forms using the well known catalytic hydrosilylation route [11, 12]:

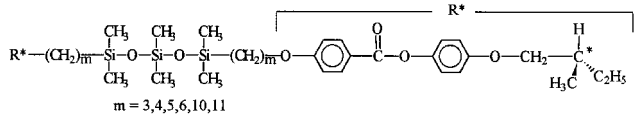

The enantiomeric form is denoted (−)*m*Dim; the racemic form is denoted (±)*m*Dim. Actually, the racemic form of the dimesogens corresponds to a mixture of diastereomers arising from the non-stereoselective hydrosilylation of the racemic mixture of the monomeric precursor. An analogous scheme is used for the monomesogens with (−)*m*Mon for the enantiomeric forms and (+/−)*m*Mon for the racemic forms. The number *m* of carbons of the alkenyl chain includes the double bonded carbon atoms.

The compounds were purified by chromatography on silica gel with toluene as eluent. The completeness of the reaction was controlled by IR spectroscopy by monitoring the disappearance of the Si–H signal at 2155 cm^{-1}. Phase characterization by POM was carried out with an Olympus BH2 microscope equipped with a Mettler FP52 hot stage. For texture observations the samples were mounted on slides without surface treatment, with the exception of the compound (−)6Dim for which commercially available liquid crystal cells (E.H.C. Co., Ltd, Tokyo) with cell gaps of 4 μm and parallel rubbed polyimide coated surfaces were used. All calorimetric studies were performed with a Perkin Elmer DSC7 calorimeter at various heating rates. The temperature dependence of the smectic layer spacing was studied using a small angle KRATKY camera equipped with a NBRAUN OED-50 one-dimensional position-sensitive detector. These experiments were carried out by a stepwise heating of the samples from room temperature to the clearing point and on cooling to room temperature again. The exposure time for each measurement amounted to 300 s. The single crystal analysis of (±)3Dim was performed with an ENRAF-NONIUS CAD4 diffractometer (MoK_α, $\lambda = 0{\cdot}71073$ Å) at room temperature (20°C).

3. Differential scanning calorimetry and polarization optical microscopy

3.1. *Phase characterization*

The phase types and sequences of the chiral dimesogens, presented in tables 1 (*a*) and 1 (*b*) were realized by POM and confirmed by DSC (heating rate ±5°C min^{-1}). All the dimesogens investigated exhibit smectic polymorphism with the exception of the homologues (−)3Dim and (−)4Dim for which no liquid crystalline behaviour is observed. For (−)4Dim, two crystalline modifications are found, showing a strong supercooling tendency of about 50°C. With increasing length of the polymethylene chain, the liquid crystallinity is promoted which agrees with a suppressed crystallization tendency. For the homologues (−)5,6,10,11Dim, microscopic observations provided characteristic liquid crystalline textures suggesting the formation of a smectic C* phase on cooling from the isotropic melt. The compounds (−)6,10,11Dim exhibit a second, more highly ordered mesophase as yet unclassified; for the compound (−)6Dim this may be a CrE*, J* or G* phase. Figure 1 depicts selected mesophase textures of the liquid crystalline dimesogens. Figures 1 (*a*) and 1 (*b*) show the different LC phases of (−)6Dim prepared in the cells with 4 μm spacing and treated surfaces. On cooling from the isotropic melt the fan-shaped texture of the SmC* phase appears and changes to the SmX* or Cr phase shown in figure 1 (*a*) at $T = 31{\cdot}9$°C. The interesting texture of (−)5Dim is derived by shearing the sample between two glass slides, figure 1 (*c*). For the compound (−)10Dim the development of the fan-shaped texture of the smectic C* phase is shown, figure 1 (*d*), growing from bâtonnets. Figure 1 (*e*) depicts the higher ordered smectic phase of (−)10Dim at lower temperatures. In figure 1 (*f*) the coexistence of fan-shaped and schlieren optical textures of the SmC* phase is presented for (−)11Dim.

3.2. *Phase transitions*

A comparative study of the phase transitions is presented by the DSC cooling and heating traces obtained with a ±5°C min^{-1} rate in figure 2. The elongation of the flexible core obviously leads to smectic mesophase broadening with increasing clearing temperatures. An odd–even effect of the clearing temperatures is detected for the first members of the homologous series of dimesogens (table 1, figure 3). The same tendency is observed for the corresponding monomesogenic precursors. A comparison of the clearing temperatures of monomesogens and dimesogens exhibits a different behaviour: while lengthening of the alkylene chain leads to an overall increase of the clearing temperatures in the case of the dimesogens, the opposite is true for the monomesogens.

The homologue (−)5Dim and its racemate show a metastable phase transition at $T \cong 23$°C on heating. Only a monotropic liquid crystalline phase is formed on cooling, and a series of DSC experiments with variable heating rates has been carried out to prove the metastability of the phase transition. A comparative study of the stable phase transitions of compound (−)10Dim and the metastable phase transitions of (−)5Dim as a

Table 1 (*a*). Transition temperatures (°C) and enthalpies (kJ mol^{-1}) in parenthesis for the enantiomeric dimesogens on cooling (DSC, 5°C min^{-1}).

Compound	I–Cr_1	Cr_1–Cr_2	I–SmC*	SmC*–SmX*	SmX*–Cr/g	SmC*–Cr
(−)3Dim	38·6 (36·9)	—	—	—	—	—
(−)4Dim	18·2 (12·7)	7·3 (16·9)	—	—	—	—
(−)5Dim	—	—	46·5 (14·4)	—	—	16·9 (8·5)
(−)6Dim	—	—	42·9 (13·4)	34·6 (0·06)	−0·6 (7·6)	—
(−)10Dim	—	—	71·3 (15·6)	11·3 (4·4)	−7·6 —	—
(−)11Dim	—	—	76·7 (16·3)	21·6 (4·6)	−0·3 —	—

Table 1 (*b*). Transition temperatures (°C) and enthalpies (kJ mol^{-1}) in parenthesis for the racemic dimesogens on cooling (DSC, 5°C min^{-1}).

Compound	I–Cr_1	Cr_1–Cr_2	I–SmC	SmC–SmX	SmX–Cr/g	SmC–Cr
(+/−)3Dim	35·4 (35·9)	—	—	—	—	—
(+/−)4Dim	18·1 (12·8)	5·8 (15·2)	—	—	—	—
(+/−)5Dim	—	—	47·1 (15·3)	—	—	16·9 8·6
(+/−)6Dim	—	—	43·8 (13·2)	35·2 (0·07)	−0·9 (5·8)	—
(+/−)10Dim	—	—	69·3 (14·6)	9·3 (4·0)	−8·6 —	—
(+/−)11Dim	—	—	77·7 (17·5)	22·4 (5·3)	−5·9 —	—

function of the heating rate is presented in figure 4. In contrast to the insignificant influence of the heating rate on stable phase transitions, a noticeable change of the metastable transition peak can be detected with increasing heating rate. Such phenomena are usually caused by kinetic effects and can easily be influenced by different sample treatments, e.g. annealing experiments. Figure 5 demonstrates the influence of duration of annealing for compound (±)5Dim at $T = 2$°C. After annealing for 3 days, a clear distinction between two stable crystalline modifications can be established.

3.3. *Crystallization tendency*

The crystallization tendency decreases with elongation of the methylene chain. The homologous compounds (−)3,4,5,6Dim and their racemic mixtures show crystallization on cooling (cooling rate: 5°C min^{-1}) as shown in the DSC cooling traces in figure 2. Under the same conditions, the compounds (−)10Dim and (−)11Dim do not crystallize at all, and rather only a glass transition is observed. The crystallization behaviour was also investigated by a series of different annealing experiments at various temperatures and durations in time. Measurements were performed in the temperature interval from −20°C to 30°C at a heating rate of 2°C min^{-1} to determine the most effective annealing temperature. A significant change of the transition only became visible by annealing at $T = 2$°C, even after a comparatively short annealing time. An annealing study at $T = 2$°C is presented in figure 6 for the compounds (±)10Dim and (±)11Dim. After annealing for one hour, a peak shift of $\Delta T = 10$°C to higher temperatures is observed for (±11)Dim, which is indicative of an increase in crystallite sizes. An annealing time of 5 months leads to a high degree of crystallinity which is confirmed by the transition enthalpy ΔH (figure 7). ΔH changes from 0·2 kJ mol^{-1} generally observed for LC–LC phase transitions, to $\Delta H = 22$ kJ mol^{-1} representing a Cr–LC phase transition. This dramatic increase may be caused by a highly ordered crystal structure for which more energy is required for transformation into the less ordered LC arrangement of the molecules than for LC–LC transitions. In addition, an increase in crystallization tendency reduces the mesophase region. In the case of compound (±)10Dim, the

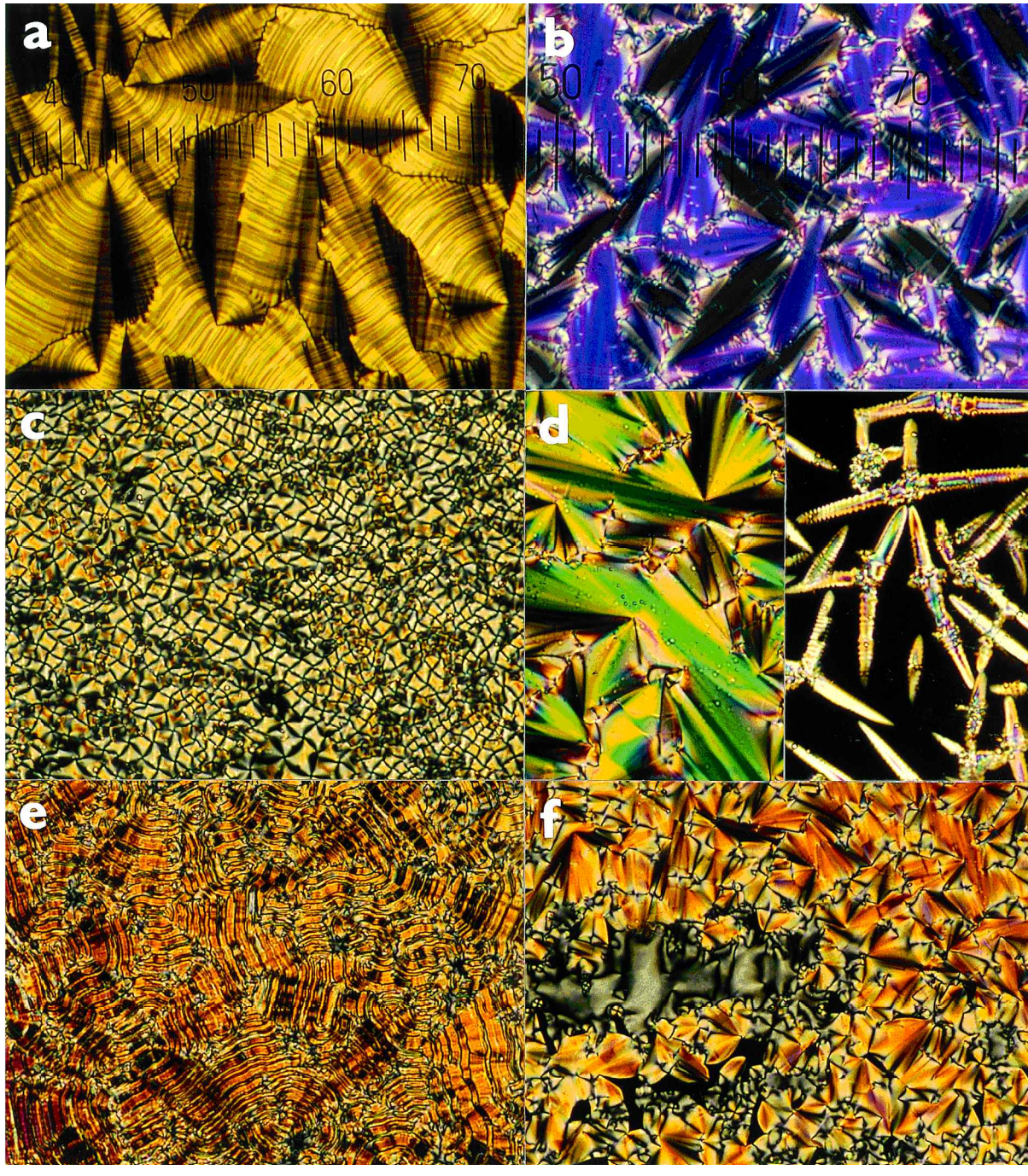

Figure 1. Characteristic textures observed for selected dimesogens: (*a*) (−)6Dim, unclassified SmX* or Cr phase ($T = 30{\cdot}9$°C, magnification 300×, possibly CrE*, CrJ* or CrG*); (*b*) (−)6Dim, SmC* phase ($T = 43{\cdot}6$°C, 470×); (*c*) (−)5Dim, interesting texture of the SmC* phase (unusual schlieren or distorted parabolic?) ($T = 46{\cdot}3$°C, 230×); (*d*) (−)10Dim, SmC* phase ($T = 69{\cdot}0$°C, 230×) grown from bâtonnets ($T = 70{\cdot}7$°C, 230×); (*e*) (−)10Dim, SmX* phase ($T = 20{\cdot}0$°C, 230×); (*f*) (−)11Dim, SmC* phase, coexistence of schlieren and fan-shaped texture ($T = 74{\cdot}6$°C, 230×).

higher ordered low temperature mesophase disappears completely after 5 months of annealing [figure 6(*b*)].

Although in comparison with the racemic systems, the pure enantiomers exhibit very similar phase and transition behaviour, differences are observed for the crystallization behaviour under the same annealing conditions and this behaviour is presented for annealing of (−)11Dim and (±)11Dim in figure 8. For the racemic system a slower crystal growth is observed and verified by experiments carried out after a shorter annealing time.

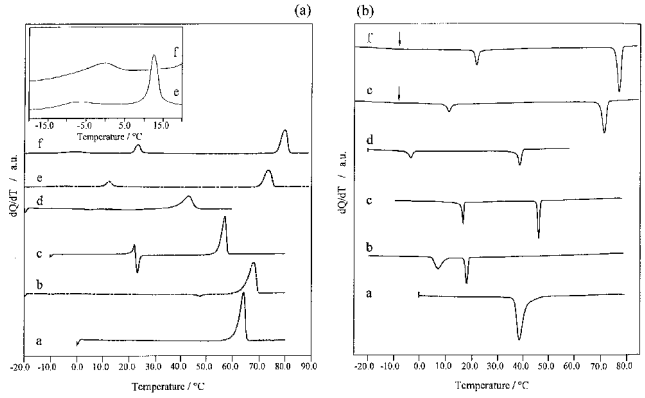

Figure 2. DSC second heating (*a*) and cooling (*b*) traces of unannealed enantiomeric dimesogens (heating rate ± 5°C min^{-1}): (a) (−)3Dim, (b) (−)4Dim, (c) (−)5Dim, (d) (−)6Dim, (e) (−)10Dim, (f) (−)11Dim.

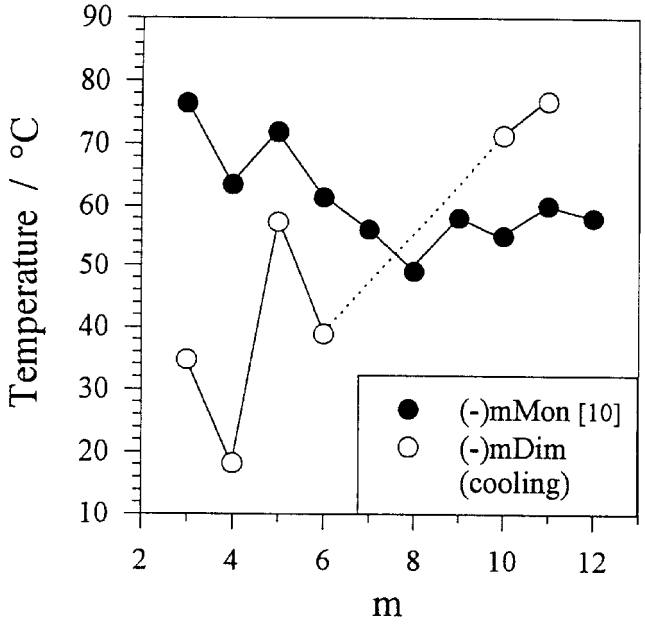

Figure 3. Clearing temperature as a function of the $(CH_2)_m$ chain length for the chiral dimesogens compared with their corresponding monomesogenic precursors [10]. All results were determined by DSC and were in agreement with optical polarizing microscopic data.

This might be explained by the different diastereomers which have to find each other to cancel dipolar packing effects, as well as to form a non-enantiomeric space arrangement. Two weeks of annealing lead to an equally developed stage of crystallization for both (−)11Dim and the racemic form.

4. Small angle X-ray (SAX) investigation

X-ray diffraction can be a helpful tool to complete the identification of liquid crystal phases in addition to POM and DSC investigations. In the case of smectic

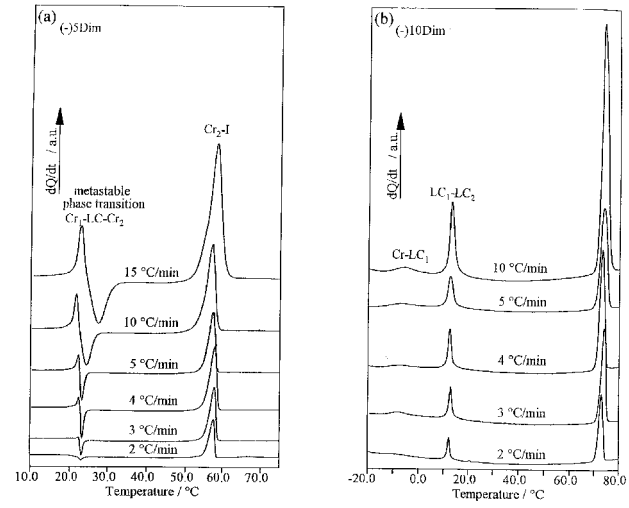

Figure 4. The metastable Cr–LC phase transition of (−)5Dim (*a*) in comparison with the stable Cr–LC and LC–LC phase transitions of (−)10Dim (*b*) as observed by DSC at variable heating rates. All samples (weight 5 mg) were heated to the isotropic phase before starting the measurements.

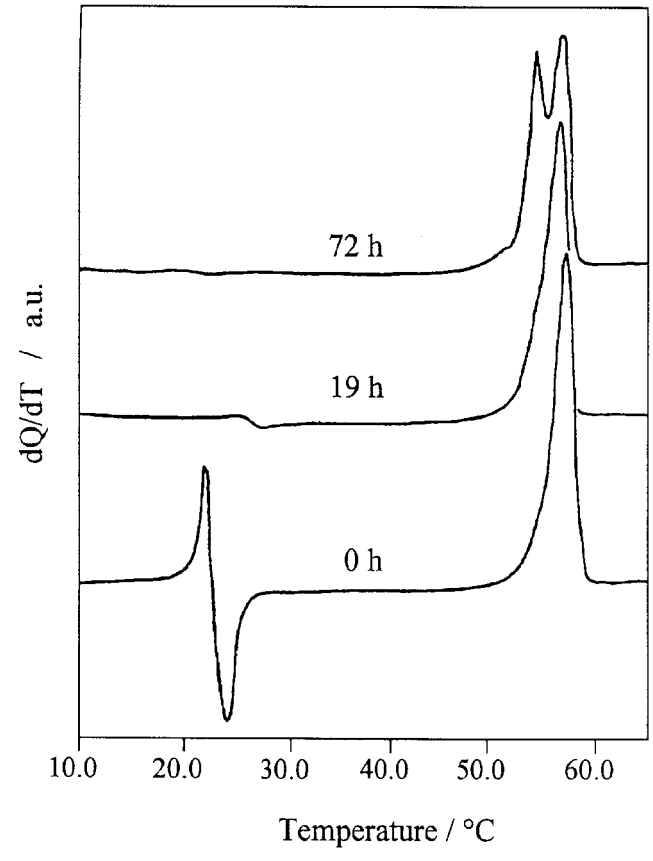

Figure 5. Influence of annealing at $T = 2$°C upon the metastable phase transition of compound (+/−)5Dim as detected by DSC (heating rate 5°C min^{-1}; sample weight 5 mg).

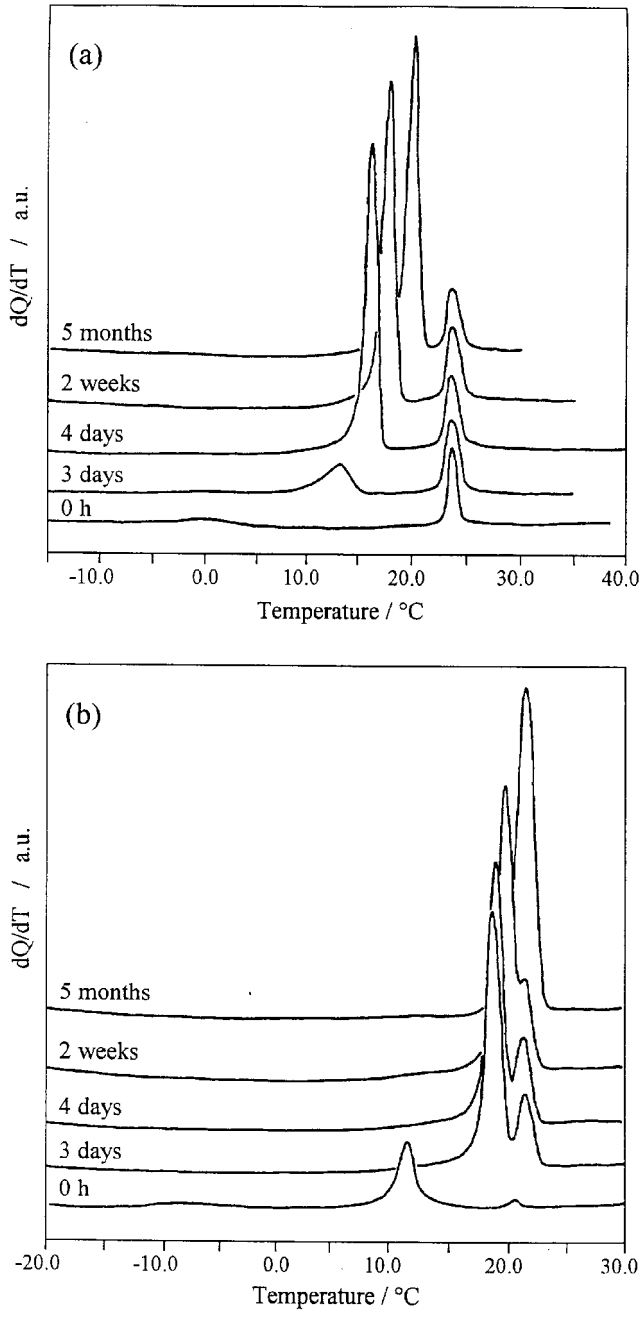

Figure 6. DSC investigation (5°C min^{-1}, 5 mg) of crystallization after different annealing durations at $T = 2$°C; (*a*) (+/−)11Dim, (*b*) (+/−)10Dim.

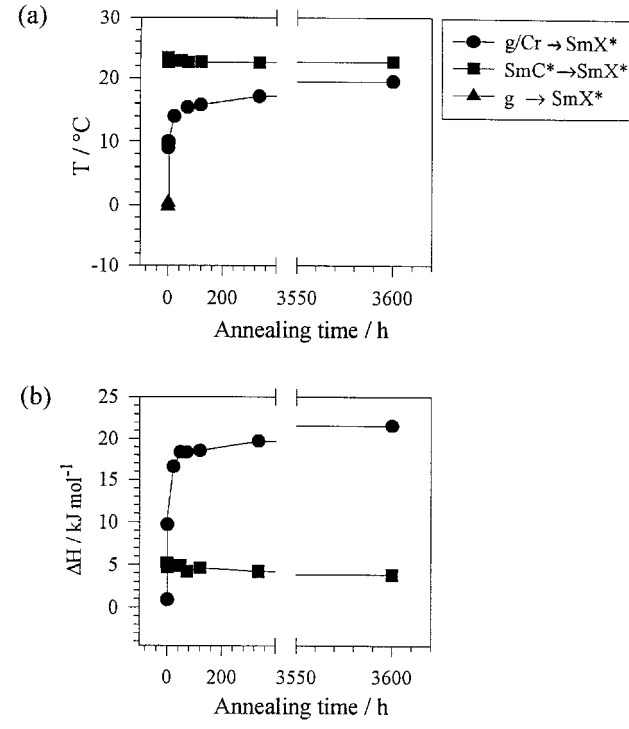

Figure 7. Transition temperature (*a*) and enthalpies (*b*) of compound (−)11Dim as a function of annealing time at $T = 2$°C.

mesophases, X-ray diffraction in the small angle region leads to the smectic layer spacing d and conclusions about the inclination of the molecules within the smectic layer. The smectic layer spacing of the monomesogens (−)10Mon and (−)11Mon is given as a function of temperature in figure 9. The phase transition smectic A* → smectic C* leads to a significant change in d value, with $\Delta d = 0{\cdot}44$ Å for (−)10Mon and $\Delta d = 0{\cdot}89$ Å for (−)11Mon which is indicative of a small tilt of the molecules in the smectic C* phase. The tilt angle φ of the molecules can be approximated by: $\cos \varphi = d_{SmC*}/d_{SmA*}$. Both materials exhibit smectic C* phases with rather small tilt angles of $\varphi = 10{\cdot}5°$ for (−)10Mon and $\varphi = 14{\cdot}2°$ for (−)11Mon.

Figure 10 presents results of a comparative study of the d spacing as a function of the methylene chain length for dimesogenic racemates and enantiomers, and their corresponding chiral mesogenic precursors at $T = 30$°C. For dimesogens as well as for monomesogens, the increasing number m of carbons in the methylene chain is reflected in a linear increase of the d value.

The lengths of the molecules are almost exactly represented by the d values of the layers in the case of the monomeric mesogens, but significant differences are observed for the dimesogens, see tables 2(*a*), 2(*b*) and 3. In the last column of these tables, the ratios listed are for the calculated fully extended conformation L using the modelling procedure by Alchemy III and the layer spacing d derived from the X-ray investigations. The d spacings for the dimesogenic enantiomers and racemates agree within the limits of experimental errors. The ratio L/d is about two for the dimesogens, dropping from above two for 3Dim to below two for the 11Dim in a similar manner for the enantiomeric and the racemic

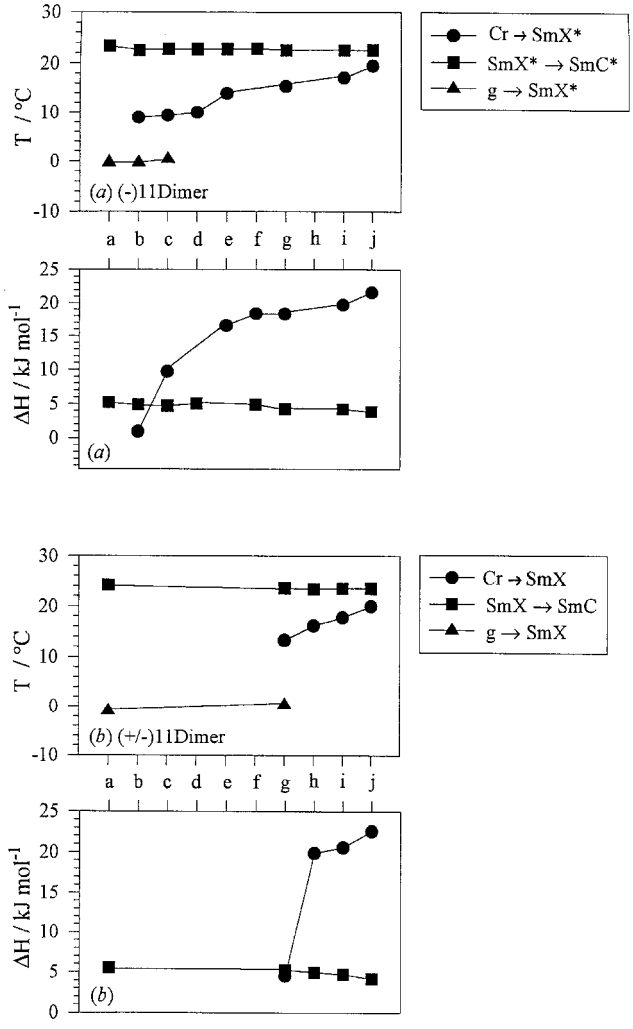

Figure 8. Crystallization behaviour of (−)11Dim (*a*) and its racemate (*b*). Annealing time at $T = 2°C$; (a) 0 h, (b) 1 h, (c) 1·5 h, (d) 2 h, (e) 24 h, (f) 48 h, (g) 72 h, (h) 96 h, (i) 2 weeks, (j) 5 months.

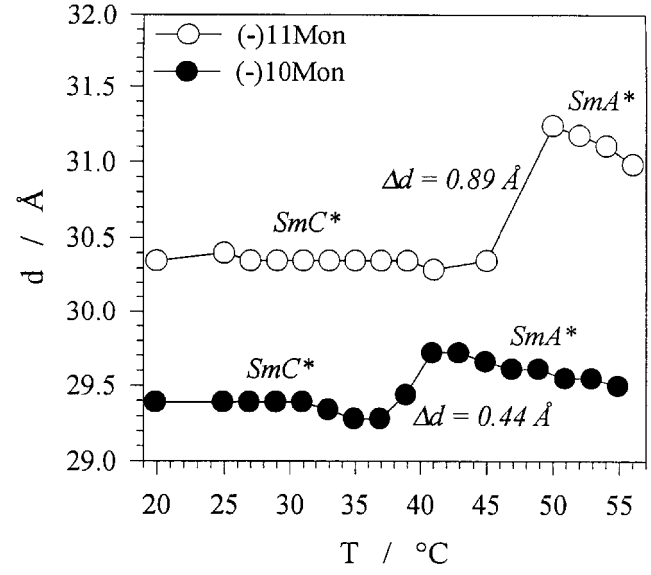

Figure 9. *d* Spacings as a function of temperature for the monomesogenic compounds (−)10Mon and (−)11Mon.

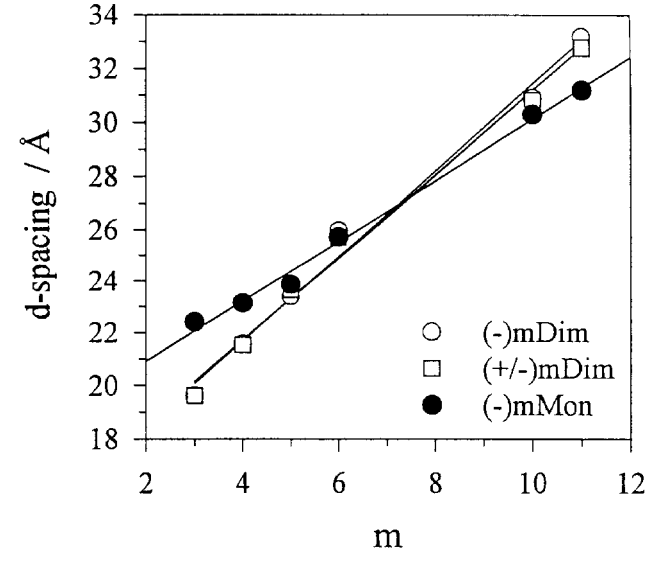

Figure 10. *d* Spacings as a function of the number *m* of carbons in the polymethylene chain of dimesogens and selected chiral monomesogens (SAX, $T = 30°C$).

compounds. This ratio is about one for the monomesogenic compounds. It is noteworthy that the ratio L/d is below one for the monomesogens, but larger than two for the dimesogens in the case of the shorter molecules.

A crystal structure determination was attempted, to obtain some insight into the experimental data. The longest dimension of the unit cell of the compound (−)11Mon [triclinic unit cell, $P1$ with $a = 5{\cdot}737\,(4)$ Å, $b = 15{\cdot}859\,(20)$ Å, $c = 30{\cdot}645\,(34)$ Å, $\alpha = 92{\cdot}27\,(7)°$, $\beta = 90{\cdot}81\,(7)°$, $\gamma = 99{\cdot}85\,(6)°$, $V = 2744\,(5)$ Å^3, four molecules within the unit cell] agrees with the *d* spacing from SAX. However, the triclinic unit cell for the (±)3Dim with $a = 13{\cdot}549\,(6)$ Å, $b = 18{\cdot}069\,(7)$ Å, $c = 23{\cdot}134\,(11)$ Å, $\alpha = 74{\cdot}45\,(3)°$, $\beta = 74{\cdot}45\,(3)°$, $\gamma = 73{\cdot}49\,(4)°$ and $V = 5127{\cdot}5\,(39)$ Å^3 cannot accommodate a fully extended chain of this compound which amounts to $L = 45$ Å. A centre of symmetry within the molecule can be excluded which could explain the dimensions obtained. A preliminary evaluation of the electron density reveals four folded strands of chains within the unit cell. The ratio of L/d of approximately two in the liquid crystalline state has then to be interpreted in terms of each dimesogen being folded, the larger ratio for the smaller molecules occurring because the folds cut off relatively more from the length of the strands for smaller molecules

Table 2(*a*). Comparison of calculated and experimental data derived from SAX for enantiomeric dimers at $T = 30°C$.

Compound	Length[a] L /Å	SAX d/Å	L/d
(−)3Dim	45·0	19·62[b]	2·29
(−)4Dim	47·4	21·57[b]	2·19
(−)5Dim	50·0	23·40[b]	2·14
(−)6Dim	52·7	25·97[b]	2·03
(−)10Dim	62·0	30·55[c]	2·00
(−)11Dim	64·6	33·19[c]	1·95

[a] Calculated length of the fully extended conformation.
[b] Crystalline.
[c] Liquid crystalline (SmC*).

Table 2(*b*). Comparison of calculated and experimental data derived from SAX for racemic dimers at $T = 30°C$.

Compound	Length[a] L /Å	SAX d/Å	L/d
(+/−)3Dim	45·0	19·62[b]	2·29
(+/−)4Dim	47·4	21·54[b]	2·20
(+/−)5Dim	50·0	23·65[b]	2·11
(+/−)6Dim	52·7	25·71[b]	2·05
(+/−)10Dim	62·0	30·80[c]	2·01
(+/−)11Dim	64·6	32·77[c]	1·97

[a] Calculated length of the fully extended conformation.
[b] Crystalline.
[c] Liquid crystalline (SmC*).

Table 3. Comparison of calculated and experimental data derived from SAX for enantiomeric monomers at $T = 30°C$.

Compound	Length L /Å	SAX d/Å	L/d
(−)3Mon	20·6[a]	22·40[b]	0·92
(−)4Mon	21·9[a]	23·10[b]	0·95
(−)5Mon	23·2[a]	23·85[b]	0·97
(−)6Mon	24·4[a]	25·71[b]	0·95
(−)10Mon	29·75[d]	29·25[c]	1·01
(−)11Mon	31·25[d]	30·30[c]	1·03

[a] Calculated length of the fully extended conformation.
[b] Crystalline, experimental data.
[c] Liquid crystalline (SmC*), experimental data.
[d] Liquid cruystalline (SmA*), experimental data.

compared with longer ones. In addition, some tilt of the molecules towards the smectic layer normal may be present. A microphase separation of siloxane units, mesogenic moieties and flexible alkyl chains [13] is not a necessity to explain the results.

The temperature dependence of the smectic layer spacing of all dimesogens investigated is illustrated in figure 11. With only one crystalline modification present, temperature independent d values were found

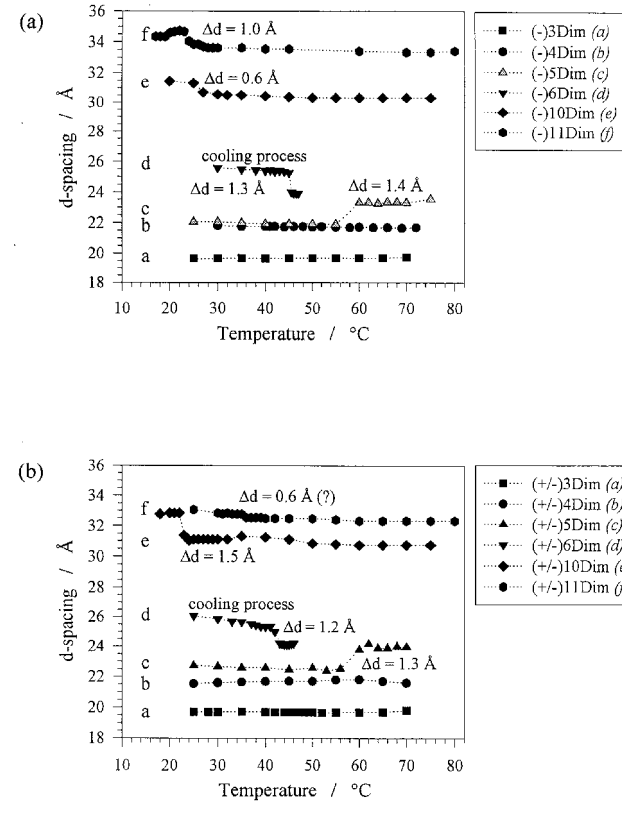

Figure 11. Temperature dependence of the d spacing derived from SAX by stepwise heating (exposure time 300 s). All samples were prepared in Mark capillaries (∅ 0·7 mm); (*a*) chiral dimesogens, (*b*) racemic dimesogens.

for (−)3Dim and (±)3Dim. The two crystalline modifications of compound (−)4Dim and its racemate detected by DSC cannot be identified by SAX by a difference in the d values, in contrast to the compounds (±)5Dim and (−)5Dim where a clear distinction is possible between the two crystalline modifications appearing at room temperature. Annealing leads to the second modification. The difference between the d values for the two modifications amounts to 1·4 Å for the pure enantiomer and 1·3 Å for the racemic system. Cooling from the isotropic melt leads directly into the liquid crystalline phase with $d = 23·1$ Å. Because of supercooling, the phase transition LC → Cr was not detected with our equipment which cannot be cooled below 20°C. A significant increase of the smectic layer spacing on cooling was observed for the compounds (±)6Dim and (−)6Dim for the monotropic SmC → SmX phase transition. The d spacing changes from $d = 24$ Å for the smectic C phase to $d = 25·2$ Å for the lower temperature phase. A similar tendency was observed for the homologues 10Dim and 11Dim at lower temperatures. Differences of the layer spacings are depicted in the graphs of figures 11(*a*) and 11(*b*).

5. Conclusions

The linkage of mesogenic units via a hexamethyltrisiloxane spacer promotes liquid crystalline behaviour. No significant differences in the transitional and structural properties were found for the enantiomeric and racemic forms.

The following conclusions concerning the dimesogenic compounds can be drawn in comparison with the related monomesogenic materials without siloxane units: all liquid crystalline dimesogens show a smectic C phase and some of them in addition exhibit a higher ordered smectic phase. A lowering of the clearing temperatures by introducing a siloxane unit in the case of the dimesogens was observed only for the shorter homologues. Results from SAX suggest a similar arrangement of the mesogens for the monomesogenic precursors and dimesogens with similar layer spacings in the smectic phases resulting from the data of a single crystal study. Chain folding is likely to occur also in the liquid crystalline state†.

† During the refereeing procedure a paper [13] appeared where a folded dimesogen was proposed as a possible model in the liquid crystalline state.

References

[1] Coles, H. J., Gleeson, H. F., Scherowsky, G., and Schliwa, A., 1990, *Mol. Cryst. liq. Cryst. Lett.*, **7,** 117.
[2] Poths, H., and Zentel, R., 1994, *Macromol. Rapid Commun.*, **15,** 433; McNamee, S. G., Bunning, T. J., McHugh, C. M., Ober, C. K., and Adams, W. W., 1994, *Liq. Cryst.*, **17,** 179.
[3] Bunning, T. J., and Kreuzer, F.-H., 1993, *TRIP.*, **3,** 318.
[4] Ibn-Elhaj, M., Skoulios, A., Guillon, D., Newton, J., Hodge, P., and Coles, H. H., 1995, *Liq. Cryst.*, **19,** 373.
[5] Cooray, N. F., Kakimoto, M., Imai, Y., and Suzuki, Y., 1995, *Macromolecules*, **28,** 310.
[6] Poths, H., Wischerhoff, E., Zentel, R., Schönfeld, A., Henn, G., and Kremer, F., 1995, *Liq. Cryst.*, **18,** 811.
[7] Bunning, T. J., Klei, H. E., Samulski, E. T., Adams, W. W., and Crane, R. L., 1993, *Mol. Cryst. liq. Cryst.*, **231,** 163.
[8] Aguilera, C., and Bernal, L., 1984, *Polym. Bull.*, **12,** 383.
[9] Kelly, S. M., Buchecker, R., and Schadt, M., 1988, *Liq. Cryst.*, **3,** 1115.
[10] Diaz, F., Valdebenito, N., Tagle, M., and Aguilera, C., 1994, *Liq. Cryst.*, **16,** 105.
[11] Lukevics, E., Belyakova, Z. V., Pomerantseva, M. G., and Voronkov, M. G., 1977, *Organomet. Chem. Rev.*, **5,** 1.
[12] Ibn-Elhaj, M., Skoulios, A., Guillon, D., Newton, J., Hodge, P., and Coles, H. J., 1996, *J. Phys. II Fr.*, **6,** 271.
[13] Corsellis, E., Guillon, D., Kloess, P., and Coles, H., 1997, *Liq. Cryst.*, **23,** 235.